Metal-induced gelation in dipyridyl ureas†

Peter Byrne, Gareth O. Lloyd, Lucas Applegarth, Kirsty M. Anderson, Nigel Clarke and Jonathan W. Steed*

Received (in Victoria, Australia) 14th April 2010, Accepted 8th June 2010
DOI: 10.1039/c0nj00278j

A series of pyridyl-appended bis(urea) ligands form supramolecular gels in the presence of metal ions (metallogels), particularly copper(II) and silver(I). The gels have been characterised by rheometry and SEM, and the effect of the metal ions on gel strength and morphology examined. The metal-induced gelation is linked to the competition between urea–urea and urea–pyridyl hydrogen bonding interactions. Crystals grown from these gels reveal a wealth of structural information about these systems that can be related to gel structure using powder X-ray diffraction data of their xerogels.

Introduction

Organogels and hydrogels made up from small molecules or 'low molecular weight gelators' (LMWGs), which are linked into fibres by supramolecular interactions are highly topical.[1–5] These materials have a wide range of potential applications in areas such as templation of nanomaterials, drug delivery and as crystal growth media.[6] Of particular recent interest is the incorporation of labile metals or anions within these supramolecular gels. Metal and anion binding can make use of self-assembly in the formation of the gelators themselves, and can also tune gel properties such as photophysics, catalytic activity, redox response and rheology.[7–10] In our group, we have focused on metal and anion tuning[11–17] of the rheological properties of the versatile bis(urea)[18–28] class of gelators. By appending metal-binding pyridyl groups to bis(ureas), the primary urea tape hydrogen bonding motif (Fig. 1a) thought to be responsible for gel fibre formation in bis(urea) gels is modulated by, or in competition with, a variety of other interactions as shown in Fig. 1. In particular, coordination interactions of the type shown in Fig. 1c can cross-link gel fibrils, increase the connectivity of each node, and hence increase gel strength. Moreover, the urea–pyridyl interaction (Fig. 1b) is also in competition with urea tape hydrogen bonding. This interaction is 'switched off' by metal binding and hence metal complexation should enhance gel strength. We now report the results of our investigations into the formation and tuning of metallogels by a range of bis(pyridylureas) shown in Scheme 1. Part of this work has appeared in preliminary form.[11]

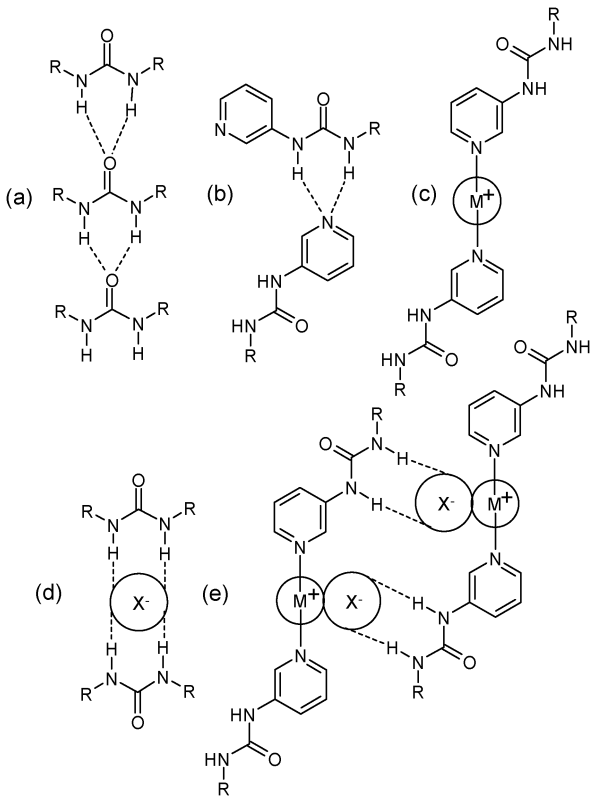

Fig. 1 Possible interactions in pyridyl urea gelators (a) urea tape, (b) urea pyridyl, (c) metal binding, (d) anion binding and (e) ion pair binding. The urea tape motif (a) is generally thought to be responsible for gel fibre formation in bis(urea) gels and is in competition with the interactions shown in (b) and (d). Metal coordination (c) reduces competition from interaction (b). Ion pair binding (e) provides an alternative possible mode of gel fibre aggregation.

Results and discussion

Ligand synthesis

Ligands $\mathbf{L^{1–13}}$ were all readily prepared by reaction of the appropriate commercial diamine with nicotinoyl azide, prepared *in situ*. Alternatively, the reaction of 3-aminopyridine with a commercial diisocyanate is equally successful. Ligands $\mathbf{L^{1–3}}$ have been reported previously.[29,30] The preparation and characterisation of $\mathbf{L^{4–13}}$ is described in the Experimental section.

Copper metallogels with $\mathbf{L^{1–9}}$

In the homologous series $\mathbf{L^{1–9}}$, none of the ligands forms gels by themselves in a range of polar solvents and solvent mixtures

Department of Chemistry, Durham University, South Road, Durham DH1 3LE, UK. E-mail: jon.steed@durham.ac.uk
† Electronic supplementary information (ESI) available: Gel pictures, additional rheology plots and pictures of apparatus. CCDC reference numbers 773253–773259. For ESI and crystallographic data in CIF or other electronic format see DOI: 10.1039/c0nj00278j

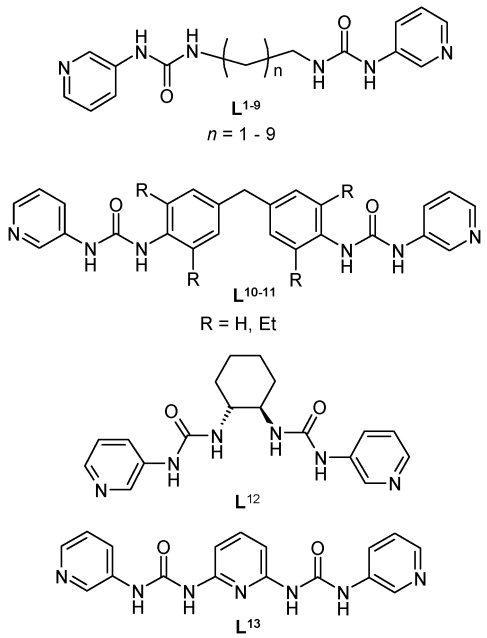

Scheme 1 Chemical structures of ligands $\mathbf{L^{1–13}}$.

(the compounds are soluble in hot aqueous methanol and hot aqueous thf). This observation contrasts to a wide range of related bis(ureas) that do not bear pyridyl substituents[18–28] and is likely to arise from the disruption of the urea tape motif (Fig. 1a) by competition with urea–pyridyl hydrogen bonding (Fig. 1b). The compounds may be crystallised from aqueous thf. X-Ray crystal structures for $\mathbf{L^{1–3}}$ have been previously reported and exhibit a gradual transition from urea $NH\cdots N_{pyridyl}$ to urea $NH\cdots O_{urea}$ tape hydrogen bonding as the alkyl chain length increases.[29] This observation suggests that gelation may be 'turned on' by metal coordination to the pyridyl groups.

On reaction with copper(II) halides, compounds $\mathbf{L^{1–6}}$ all form blue-green metallogels in mixtures of water and thf at various ratios. In contrast, the formation of viscous liquids was observed for copper(II) chloride complexes of $\mathbf{L^{7–9}}$.

When one equivalent of copper(II) chloride is added to cold solutions of *N*,*N*″-ethylene-1,2-diylbis(*N*′-pyridin-3-ylurea) ($\mathbf{L^1}$) (1 wt%) in a water and thf mixture (3 : 2), an opaque green gel forms as shown in Fig. 2. The gel is not thermoreversible and gradually loses solvent upon heating. Varying the ratio of copper(II) chloride to $\mathbf{L^1}$ suggests that a 1 : 1 ratio is optimal for gel formation, Fig. 3. At half an equivalence of

Fig. 2 Metallogel formed from the reaction of $\mathbf{L^1}$ with one equivalent of copper(II) chloride in H_2O/thf (3 : 2) at 1 wt%.

Fig. 3 Copper(II) chloride gels formed with $\mathbf{L^1}$ in varying ratios; left to right, copper(II) chloride: $\mathbf{L^1}$ ratios 0.5 : 1, 1 : 1, 2 : 1, 4 : 1 and 8 : 1.

copper(II) chloride, a clear partial gel that is formed may be due to the low concentration of gel fibres. Addition of one equivalence of copper(II) fully gels the solvent and the mixture becomes more opaque, suggesting some crystallisation to give larger particles. Additional copper(II) chloride weakens the gel again and ultimately results in a precipitate within a liquid mother liquor. These results implicate a complex of 1 : 1 stoichiometry as the gelator species, likely to be a linear, 1D coordination polymer $[Cu(S)_4(\mathbf{L^1})]_n$ (S = solvent). Addition of further metal salt may reduce the ability of this material to gel because of hydrogen bonding of the urea moieties to the chloride anions, in a way seen for related metallogels and anion-inhibited bis(urea) gels.[14,15] The gels are non-thermoreversible, suggesting that the gel is a kinetic product.

The effect of changing the thf to water ratio was investigated (Fig. 4), and it was found that gels form from a 1 : 1 mixture of $\mathbf{L^1}$ and copper(II) chloride in solvent mixtures of ratios ranging from 4 : 1 to 1 : 1 (water : thf). Why gels form in this range may be related to the optimum solubility balance of the gelator complex. In pure thf a significant colour change to give an orange precipitate is observed suggesting the formation of a different type of coordination complex and highlighting the possible involvement of water in the coordination sphere of the gelator. Competition between gelator and crystalline coordination complexes has been observed in previous work on related systems.[14]

The infra-red spectrum of $\mathbf{L^1}$ contains peaks assigned to ν(C=O) and N–H bending at 1640 and 1549 cm^{-1}, respectively. This may be compared to 1616 and 1554 cm^{-1} in the copper(II) chloride xerogel obtained by drying a gel derived from a 1 : 1 mixture of $\mathbf{L^1}$ and copper(II) chloride in 3 : 2 water : thf. These observations are consistent with increased urea hydrogen bonding in the xerogel.[31,32] Samples of the copper(II) chloride gel were dried under vacuum, coated with chromium and examined using scanning electron microscopy. Fig. 5 is a micrograph of the xerogel and shows fibres less than 50 nm wide and up to 500 nm long. The fibrous nature of the sample is consistent with gel formation.[33]

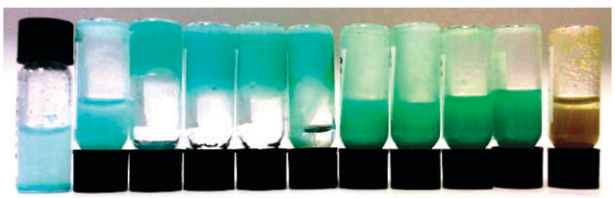

Fig. 4 Metallogels and precipitates formed from $\mathbf{L^1}$ and $CuCl_2{\cdot}2H_2O$ in water : thf mixtures from left to right: 10 : 0, 9 : 1, 8 : 2, 7 : 3, 6 : 4, 5 : 5, 4 : 6, 3 : 7, 2 : 8, 1 : 9 and 0 : 10.

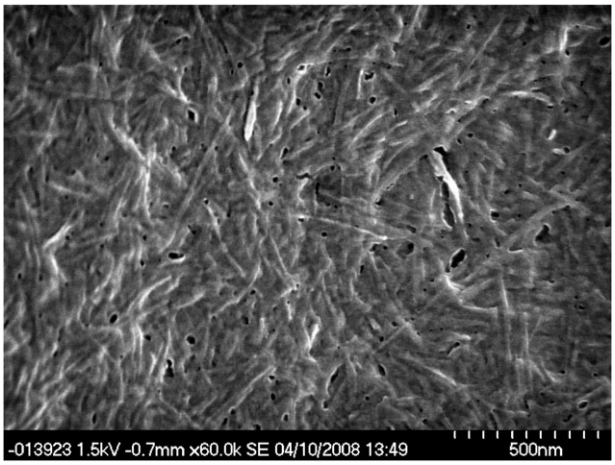

Fig. 5 SEM micrograph of a xerogel prepared from $\mathbf{L^1}$ and copper(II) chloride (1 : 1, 1 wt%) from water : thf (3 : 2).

In contrast to copper(II) chloride, reaction of $\mathbf{L^1}$ with copper(II) bromide in aqueous thf does not result in full gels, although gel-like viscous liquids do arise. A dried sample of this viscous liquid obtained under similar conditions as the image in Fig. 5 is shown in Fig. 6. The apparent larger and shorter fibres present suggest that the underlying self-assembly of a fibrous aggregate is similar to the chloride case, however interactions to the chloride anions enhance gel strength and fibre length, while reducing crystallinity.

The copper(II) chloride gel of $\mathbf{L^1}$ was probed by stress sweep rheometry at a variety of concentrations using a concentric cylinder couette. The concentric cylinder geometry proved more effective at handling weak gels or partially gelled solutions. A representative experiment is shown in Fig. 7a. The rheometry data clearly establish the solid-like nature of the gel with G' *ca.* one order of magnitude greater than G''. At 0.5 wt% the gel does not form and hence G' is very low. At 0.75–1.25 wt% G' is *ca.* 1 kPa, rising to *ca.* 8 kPa at 2 wt%. There is a clear underlying trend of increasing gel strength with increasing gelator concentration, however, the gel's lack of thermoreversibility and the relatively poor reproducibility of

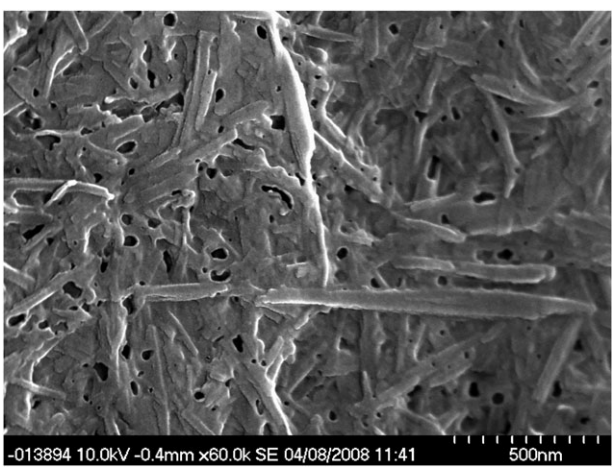

Fig. 6 SEM micrograph of a dried sample of a partial gel prepared using $\mathbf{L^1}$ and copper(II) bromide.

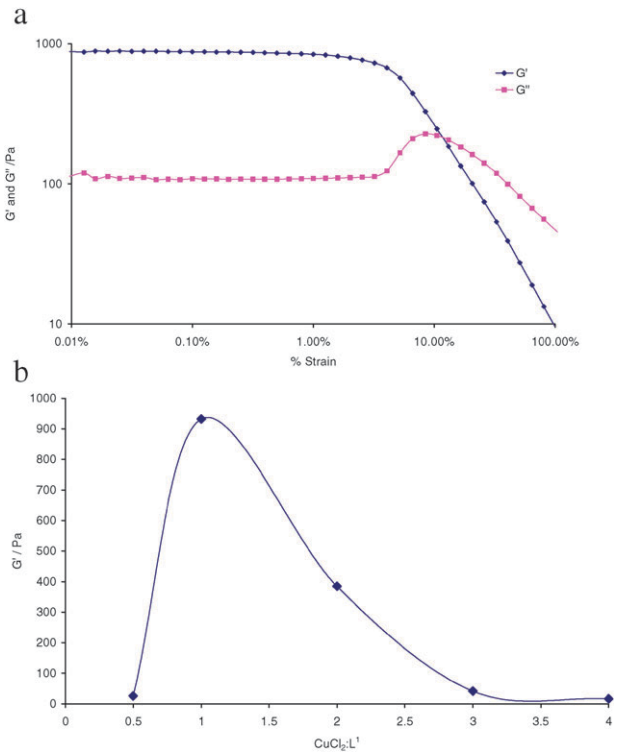

Fig. 7 (a) Stress sweep rheometry for a 1 : 1 $CuCl_2$: $\mathbf{L^1}$ metallogel (1 wt%) in a mixture of water/thf (3 : 2 v/v). (b) Elastic modulus for copper(II) chloride gels as a function of copper concentration (average of two runs).

the absolute values means that it is not possible to determine the concentration dependence quantitatively. The increase in G'' near the gel yield point is suggestive of viscoelastic properties involving a change in underlying gel structure and/or connectivity under stress.[34] Experiments over a range of copper : ligand ratios clearly establish a 1 : 1 ratio as being most favourable for optimum gel formation, Fig. 7b. A temperature sweep at a constant strain of 5% was performed to determine the gel–sol (T_{gel}) phase transition temperature. As the temperature is raised at 5 °C min^{-1}, there is no clear temperature at which G'' becomes larger that G' to indicate liquid-like behaviour, however there is a general decrease in the gel strength, indicated by the decrease in G' up to the boiling point of thf at approximately 66 °C.

Similar gels were observed upon addition of copper(II) chloride to ligands $\mathbf{L^{2-6}}$ with no systematic dependence of gel strength on the length of the oligomethylene spacer, within the limitations of the rheological measurements. However, no gels formed for spacers with $n > 6$, and instead viscous liquids resulted. In addition to water/thf mixtures, it proved possible to gel aqueous acetonitrile (1 : 1 v/v) and thf, acetonitrile and water mixtures (1 : 1 : 1 v/v), however the ligands are not fully soluble in single component solvents. In these mixed solvents more transparent gels resulted suggesting lower crystallinity. In general gels formed at similar minimum gelator concentrations to thf/water gels of copper(II) chloride and $\mathbf{L^1}$ and exhibited similar elastic moduli and yield stress, without any obvious trend.

Reaction of $\mathbf{L}^{2-6}$ with copper(II) bromide in general results in weaker gels compared to the chloride analogues, or in viscous liquids. However, in the most optimal case $\mathbf{L}^{5}$ (hexamethylene spacer) does form a robust, transparent blue gel with copper(II) bromide in a three component mixture of thf, acetonitrile and water (1 : 1 : 1 v/v) at 1 wt%, Fig. 8. Frequency sweep rheometry showed the gel to have a reproducibly moderately high elastic modulus with a plateau of 7 kPa that is invariant with frequency confirming solid-like characteristics. An SEM micrograph of the xerogel shows a fibrous structure with relatively short, homogeneous fibres *ca.* 100 nm in width.

Reaction of $\mathbf{L}^{1-9}$ with other copper(II) salts, namely nitrate, acetate and sulfate, did not result in any gel formation and instead resulted generally in precipitation. Similarly no gels were formed with other first row transition metal salts and instead precipitates resulted suggesting binding of the metal to the ligand. It may be that the particular combination of copper(II) (with its tendency to form labile four-coordinate structures) and particular anions represents the optimum liability/stability balance for gel formation, whereas more strongly hydrogen bonding anions destroy gel structure. In the case of the reaction of $\mathbf{L}^{1}$ with copper(II) nitrate in aqueous thf the solid precipitate was characterised by X-ray crystallography, Fig. 9. The data revealed a linear 1 : 1 coordination polymer of formula $\{[Cu(\mathbf{L}^{1})](NO_3)_2{\cdot}6H_2O\}_n$, (**1**) consistent

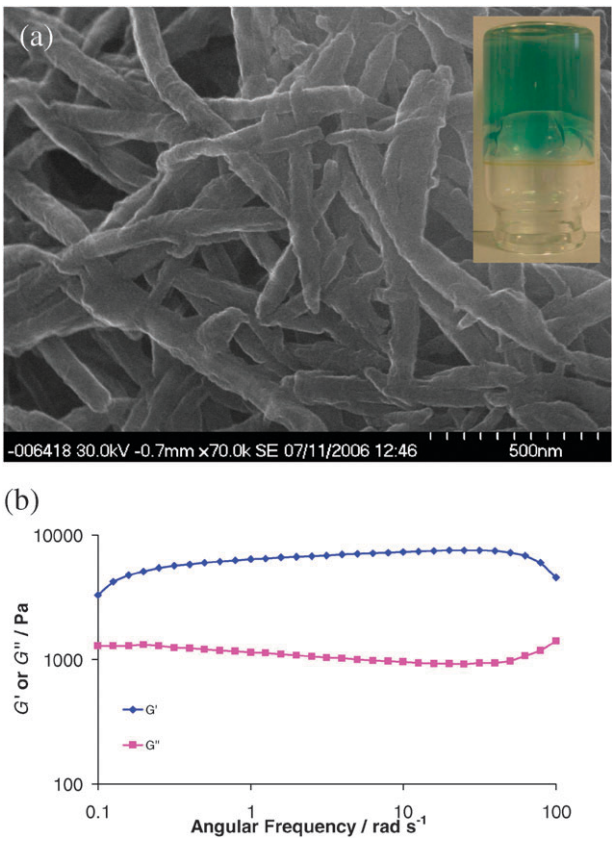

Fig. 8 Metallogel arising from a 1 wt% mixture of $\mathbf{L}^{5}$ and copper(II) bromide (1 : 1 ratio) in thf/acetonitrile/water mixed solvent (a) SEM micrograph of the xerogel with inset image of the gel and (b) frequency sweep gel rheometry.

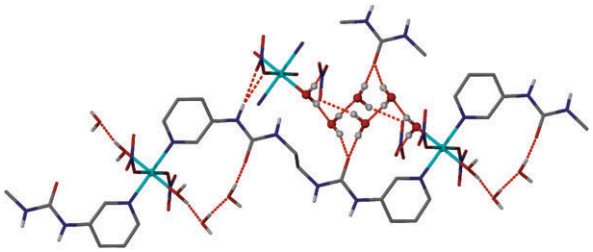

Fig. 9 X-Ray crystal structure of $\{[Cu(\mathbf{L}^{1})](NO_3)_2{\cdot}6H_2O\}_n$ (**1**) showing the 6-membered water cluster (small spheres) and the unusual $R_1^2(4)$ hydrogen bonded motif (CH hydrogen atoms omitted for clarity).

with the 1 : 1 optimal stoichiometry observed for the copper(II) chloride gelator analogue. The asymmetric unit comprises half of the formula unit and the copper atom and the $\mathbf{L}^{1}$ ligand lie on independent inversion centres. The urea NH group closest to the aryl ring binds to an adjacent nitrate anion in an unusual bifurcated donor hydrogen-bond, while the other urea NH group remains essentially unbound with the closest N···O contacts in excess of 3.4 Å. The urea oxygen is hydrogen-bonded to a six-membered water cluster, two members of which coordinated to the copper(II) centres, *trans* to a water ligand of an adjacent cluster. Along with the two molecules of water, the coordination sphere of the Jahn–Teller distorted octahedral copper(II) centre is also bound to two pyridyl nitrogen atoms of two different $\mathbf{L}^{1}$ ligands and two nitrato anions. The urea tape hydrogen bonded motif is absent in the structure since the urea NH groups interact in an unusual fashion with coordinated anions (the $R_2^2(8)$ hydrogen bonded ring is much more common than the present $R_1^2(4)$ motif[35]). While this crystalline complex is not itself a gelator, it represents a plausible model for the chloride analogue, particularly with regard to the inclusion of a large amount of solvent water, the pyridyl coordination, stoichiometry and interactions to anions.

Silver(I) metallogels with $\mathbf{L}^{1-9}$

When a solution of $\mathbf{L}^{1}$ in water and thf (3 : 2) is added to silver(I) nitrate and sonicated, the metal salt dissolves to a clear solution, and on further sonication, a colourless gel is formed. Without the extended sonication, a white solid precipitates and no gel forms. Similarly gelation does not occur on heating and cooling. Sonication has been used in the preparation of a number of gel samples that do not form in its absence.[16,36–38] The infra-red spectra of a xerogel of compound $\mathbf{L}^{1}$ with silver(I) nitrate was recorded and compared to that from the free ligand. In the free ligand, peaks corresponding to the C=O stretch and N–H bend occur at 1640 and 1549 cm^{-1}, respectively, and in the dried gel, they are shifted to 1614 cm^{-1} and the NH at 1557 cm^{-1} consistent again with a hydrogen-bonded urea. We attempted to determine the T_{gel} value, but as with the copper(II) gels, the gel is not thermoreversible and loses solvent upon heating. The tertiary structure of the gel was examined using SEM. Compared to the copper(II) chloride and bromide gels, the xerogel structure formed with silver(I) nitrate (shown in Fig. 10) is very different in appearance. The fibres are approximately 50 nm wide and over 10 μm long with an overall more well defined and more extensively

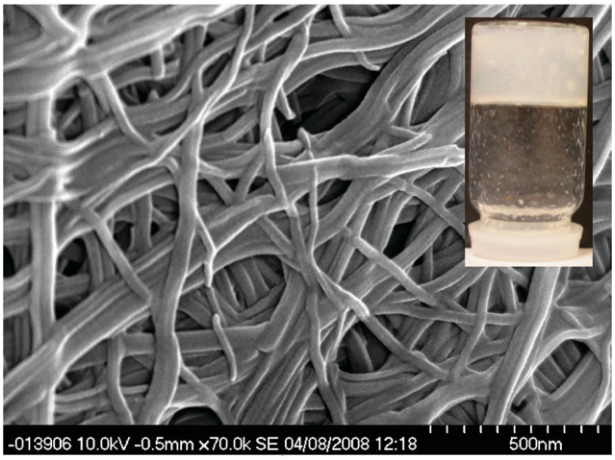

Fig. 10 Gel formed from $\mathbf{L^1}$ in water and thf (3 : 2) with silver(I) nitrate: SEM micrograph and image of the gel (inset).

interconnected network. Despite this well defined network, however, stress sweep rheometry indicates that the gel is relatively weak with G' only *ca.* half an order of magnitude greater than G'' at 2 wt%, and the gel flowing at relatively low applied stress, Fig. 11. The elastic modulus appears to scale with the square of gelator concentration although the non-thermoreversible and relatively fragile nature of the gel makes quantitative measurements difficult.

The chemical structure of the fibres formed in the gel between $\mathbf{L^1}$ and silver(I) nitrate is not known, although extensive data on a range of related compounds suggest a silver(I) ion coordinated by the pyridyl functionalities with hydrogen bonding of the urea NH groups to nitrate counter ions.[39–43] Variation of solvent systems resulted in the isolation of two types of crystalline product from the reaction of $\mathbf{L^1}$ with $AgNO_3$, one that forms directly from the aqueous thf gel upon standing. The first product arises from crystallisation of $\mathbf{L^1}$ from a mixture of acetonitrile, chloroform and methanol (3 : 3 : 4) in the presence of silver(I) nitrate. This procedure gives diffraction quality crystals within *ca.* five minutes at room temperature. The structure was determined using X-ray crystallography and was shown to be a [2 + 2] metallomacrocycle of formula $[\{Ag(\mathbf{L^1})(MeCN)\}_2](NO_3)_2{\cdot}CHCl_3$ (**2**) shown in Fig. 12. Half of the macrocycle is crystallographically

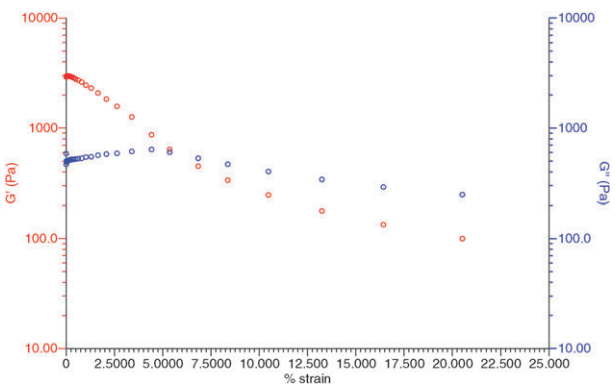

Fig. 11 Stress sweep rheometry for a 1 : 1 gel of $AgNO_3$ and $\mathbf{L^1}$ in aqueous thf, 2 wt%.

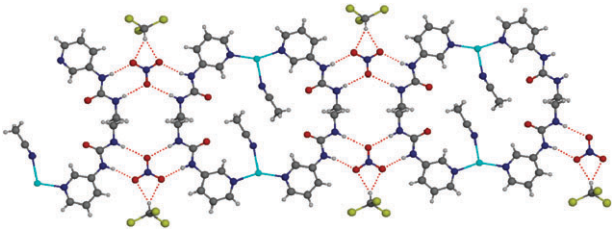

Fig. 12 X-Ray crystal structure of the metallomacrocycle $[\{Ag(\mathbf{L^1})(MeCN)\}_2](NO_3)_2{\cdot}CHCl_3$ (**2**).

unique and is situated upon a crystallographic inversion centre. Each silver(I) ion is bound to two pyridyl nitrogen atoms, with a longer bond to an acetonitrile solvent molecule such that the two molecules of acetonitrile fill the macrocycle cavity. Individual macrocycles are linked together by a double $R_2^2(8)$ hydrogen bonded ring motif[44,45] with the remaining face of the nitrate anions hydrogen bonding to the chloroform CH group.

Upon standing a gel sample prepared by sonication of a mixture of $\mathbf{L^1}$ and $AgNO_3$ in aqueous thf a second type of crystal was obtained which proved to be a remarkable Borromean weave coordination polymer of 2 : 3 Ag : $\mathbf{L^1}$ stoichiometry, formula $[Ag_2(\mathbf{L^1})_3](NO_3)_2{\cdot}7H_2O$ (**3a**), Fig. 13. The structure of this fascinating material has been described in detail elsewhere[46] and involves saturated hydrogen bonding from urea NH groups to nitrate anions as well as a discrete 7-membered water cluster.

Interestingly, repetition of the crystallisation of metallomacrocycle **2** at half of the concentration gives another Borromean structure—a pseudopolymorph of the system shown in Fig. 13—of formula $[Ag_2(\mathbf{L^1})_3](NO_3)_2{\cdot}2MeCN{\cdot}x$S (**3b**), where S is a disordered solvent, likely to be an occluded

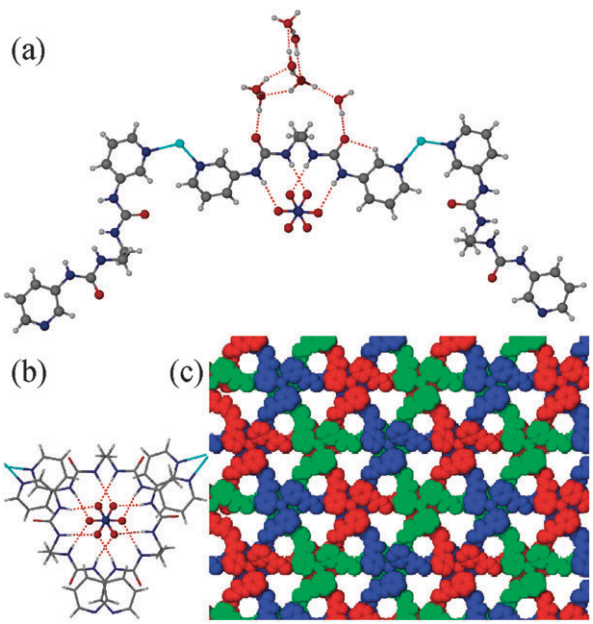

Fig. 13 X-Ray crystal structure of $[Ag_2(\mathbf{L^1})_3](NO_3)_2{\cdot}7H_2O$ (**3a**) (a) asymmetric unit (b) nitrate hydrogen bonding environment and (c) Borromean weave comprising three independent coordination polymeric networks.[46]

2 : 1 mixture of $CHCl_3$ and methanol.[46] Since the solvent mixture used in the crystallisation of **2** and **3b** is identical with **3b** produced at lower concentration it is likely that **2** is a kinetic product, while **3b** is the thermodynamic product.

To determine the relationship between the gel and the single crystal structures of **2** and **3a** we compared the X-ray powder diffraction patterns of the single crystals, the bulk precipitate isolated from the gelation mixture without sonication and the dried xerogel, Fig. 14. There is a clear match between powder and xerogel and both exhibit strong similarities to the pattern of **2** (which is obtained from a different solvent) and it is therefore likely that a solvate of the kinetic product, metallo-macrocycle **2** is related to the structure of the gelator, with the material converting to the thermodynamic Borromean structure over time. Extensive experimentation in different solvent systems has resulted in a total of five pseudopolymorphic Borromean structures in this system and full details will be reported elsewhere.

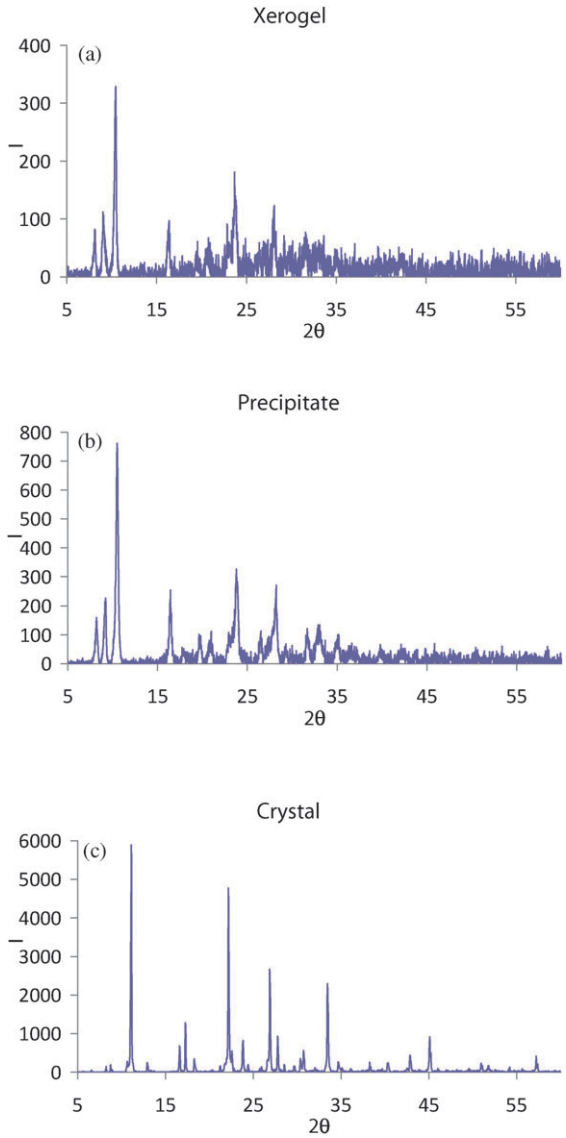

Fig. 14 (a) Experimental PXRD pattern (Cu-K_α) for the dried xerogel obtained from $AgNO_3$ and $\mathbf{L^1}$, (b) precipitate obtained from the same reaction without sonication and (c) crushed single crystals used in the determination of the structure of **2**.

Reactions of $\mathbf{L^1}$ with a range of other soluble silver(I) salts were undertaken in a variety of polar solvent mixtures without the isolation of additional gels. Instead the systems display a strong tendency to crystallise as 1D coordination polymeric products and species of formulae $\{[Ag(\mathbf{L^1})](OAc)\cdot 4H_2O\}_n$ (**4**), $\{[Ag(\mathbf{L^1})](SiF_6)_{0.5}\cdot dmf\}_n$ (**5**) and $\{[Ag(\mathbf{L^1})](BF_4)\cdot MeOH\}_n$ (**6**) were isolated from the reactions with silver acetate (**4**) and tetrafluoroborate (**5** and **6**), and characterised by X-ray crystallography. Compound **5** presumably arises from the leaching of silicate from the glass container by residual HF formed from the BF_4^- anion.

Of these salts, compound **6** is highly informative about the interplay between coordination and hydrogen bonding interactions in these pyridyl urea systems and represents an elegant conceptual model of the target gel structure. The structure comprises two independent half $\mathbf{L^1}$ ligands, each lying about independent inversion centres, linked by two-coordinate Ag(I) ions into a linear 1D coordination polymer (Fig. 15) and hence the pyridyl nitrogen atoms are unavailable for the mixed bifurcated urea $NH\cdots N_{pyridyl}$ hydrogen bonding seen in the structure of the free ligand.[29] As a result the coordination polymer chains form an antiparallel double urea tape arrangement linking chains together into a 2D sheet. The urea hydrogen bonding is apparently optimal, with all four independent $NH\cdots O$ distances short and in the narrow range 2.84–2.85 Å. The methanol molecule forms a very long contact of 2.78 Å to the Ag(I) ion and hydrogen bonds to the BF_4^- anion. This double antiparallel arrangement is typical for bis(urea) gelators, whereas a parallel arrangement is seen for non-gelators,[15] and highlights the role of the metal in removing the possibility of competing urea–pyridyl interactions as well as cross-linking hydrogen bonded fibres.

The hexafluorosilicate structure (**5**) contrasts sharply with that of **6** in that the urea tape motif is entirely absent. The ligand adopts a curved conformation different to both **6** and the structure of free $\mathbf{L^1}$, with both urea groups orientated in the same direction and hydrogen bonding only to the SiF_6^{2-} anions (Fig. 16). Each anion accepts a total of eight $NH\cdots F$

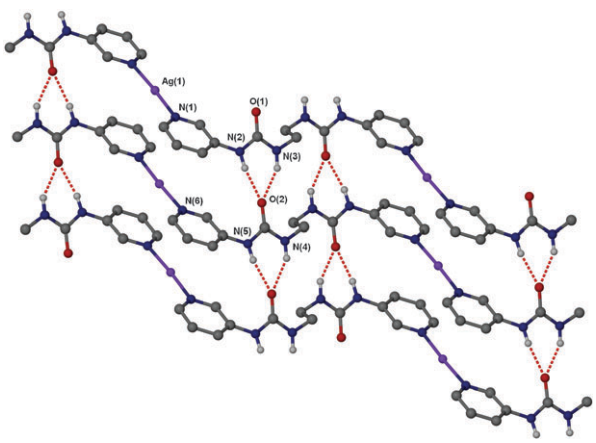

Fig. 15 X-Ray crystal structure of $\{[Ag(\mathbf{L^1})](BF_4)\cdot MeOH\}_n$ (**6**) showing the urea tape hydrogen bonding motif (CH hydrogen atoms, counter ion and solvent omitted for clarity).

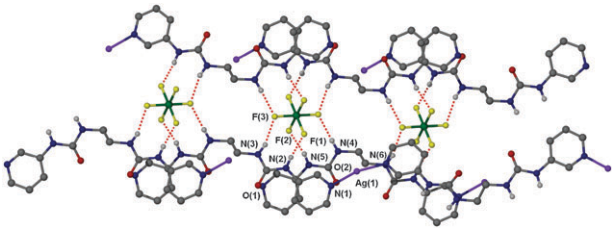

Fig. 16 X-Ray crystal structure of $\{[Ag(\mathbf{L^1})](SiF_6)_{0.5}\cdot dmf\}_n$ (**5**) showing the urea–anion hydrogen bonding motif (CH hydrogen atoms and solvent omitted for clarity).

interactions such that it is entirely surrounded by four $R_2^2(8)$ hydrogen bonded rings. The SiF_6^{2-} anions thus bridge between 1D coordination polymer chains in a 3D fashion. The unusual conformation of $\mathbf{L^1}$ probably arises from charge balance considerations and hence the dearth of hydrogen bond acceptor anions, resulting in a need to maximise the number of NH donors around each dianion. While SiF_6^{2-} is not a particularly strong hydrogen bond acceptor, the double charge makes it competitive with the urea carbonyl hydrogen bond acceptor, in contrast to non-coordinating monovalent perfluoro anions such as BF_4^-. This structure highlights the ability of anions to interfere with the urea tape hydrogen bonding motif (*cf.* Fig. 1a and d). The dmf solvent molecule is loosely interacting with the silver ion in a similar way to **6**.

The acetate structure **4** represents an interesting mixture between urea tape type and urea–anion type hydrogen bonding that appears to be related to the excess of urea NH donors over acetate acceptor atoms (Fig. 17). The 1D coordination polymer strands involve an all-*trans* ligand conformation different from both the *gauche* conformation found in free $\mathbf{L^1}$ and **6** and the curved conformation in **5**. Discrete pairs of coordination polymer strands are linked by a discrete, antiparallel pairwise urea···urea $R_2^1(6)$ motif (as in the infinite urea tape) but these pairs are then terminated by a capping urea···acetate $R_2^2(8)$ interaction. The lattice water forms an extensive, ordered network that links between coordination polymer strands.

Related structures with $\mathbf{L^4}$ as well as a fascinating quintuple helical structure arising from the reaction of $\mathbf{L^4}$ and $AgBF_4$ have been reported elsewhere.[47]

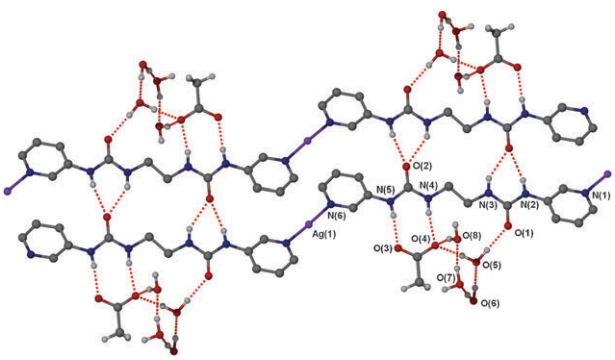

Fig. 17 X-Ray crystal structure of $\{[Ag(\mathbf{L^1})](OAc)\cdot 4H_2O\}_n$ (**4**) showing the urea–urea and urea–anion hydrogen bonding motif (CH hydrogen atoms on $\mathbf{L^1}$ omitted for clarity).

Metallogels from $\mathbf{L^{10}}$–$\mathbf{L^{11}}$

Ligand $\mathbf{L^{10}}$, *N*,*N*″-methylenebisphenyl-4,1-diylbis(*N*′-pyridin-3-ylurea) proved to act as a hydrogelator for water/thf mixtures even in the absence of metal ions with the optimum solvent composition being 3 : 2 thf : water, at concentrations down to 1 wt%. The gels proved to be relatively weak, however and opaque, indicating larger particle size and hence a high degree of crystallisation or aggregation. Addition of both $AgBF_4$ and $AgNO_3$ gives significantly stronger gels that are stable as low as 0.2 wt% in the same solvent. The T_{gel} of the systems (1 wt%) was measured by warming a sealed, inverted sample tube completely submerged in a stirred water bath in order to minimise evaporation. Under these conditions T_{gel} increased significantly from 21 °C at 0.5 equivalents of $AgBF_4$ to a plateau value of 41 ± 2 °C at one equivalent of $AgBF_4$. This value then remained constant upon addition of further metal salt (ESI†, Fig. S1). Similar results were observed for $AgNO_3$ with a value of 40 °C at one equivalent. The T_{gel} continued to rise to 45 °C at 1.5 equivalent but then decreased to 36 °C between one and two equivalents. After two equivalents the temperature rose again to 44 °C (average of three runs). We interpret these data as arising from optimum gelation at 1 : 1 ratio with increasing T_{gel} as a function of time resulting from gel maturation, balanced against the effect of excess NO_3^- decreasing T_{gel} because of interfering hydrogen bonding to the urea groups. The optimal 1 : 1 ratio obtained at least with the non-coordinating anion is consistent with the structure of **6**, *vide supra*.

In the case of thf/water silver metallogels of $\mathbf{L^{10}}$ the gels proved to be thermoreversible and undergo interesting visual changes upon cooling from above the T_{gel}. Cooling a mixture of $AgNO_3$ and $\mathbf{L^{10}}$ in 8 : 5 v/v water/thf in a water bath over *ca.* six hours results initially in the formation of an opaque, white gel at 34 °C after 10 minutes cooling from a solution initially at 57 °C. Interestingly this gel gradually clears and transforms into a transparent, colourless gel over *ca.* 5 hours at room temperature. These results suggest the initial formation of a crystalline gelatinous precipitate that transforms (probably by redissolution) into a more stable metallogel phase, Fig. 18.

When an equivalent of silver(I) nitrate is added to a solution of $\mathbf{L^{10}}$ in water and thf (2 : 3), the solution turns into a clear, colourless gel in a similar way to the system shown in Fig. 19a. After twenty-four hours, crystal growth begins within the gel resulting in colourless needles within a gel matrix, Fig. 19b. The crystalline sample of formula $[\{Ag(\mathbf{L^{10}})(thf)\}_2](NO_3)_2\cdot 4thf$ (**7**) was characterised by X-ray crystallography, Fig. 20. The structure comprises a metallomacrocycle similar to **2** (*cf.* Fig. 12) formed from two molecules of $\mathbf{L^{10}}$ and two silver(I) ions

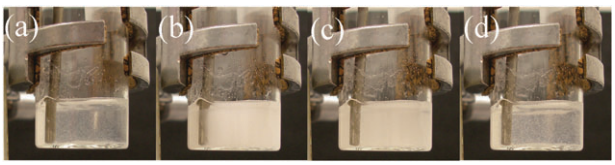

Fig. 18 Time-lapse photographs of the cooling of a 1 : 1 mixture of $\mathbf{L^{10}}$ and $AgNO_3$ in water/thf 8 : 5 v/v. (a) Initial solution, 57 °C, (b) gelation at 10 min, 34 °C, (c) cooling to room temperature 22 °C at 70 min and (d) clear gel after 320 min.

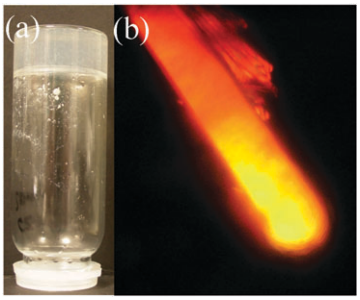

Fig. 19 (a) Gel sample obtained from $\mathbf{L^{10}}$ and $AgNO_3$ (1 : 1) in thf/water (3 : 2 v/v) upon standing for one week and (b) same sample viewed through a polarised optical microscope showing colourless crystals within the gel (the orange colour is a light scattering effect).

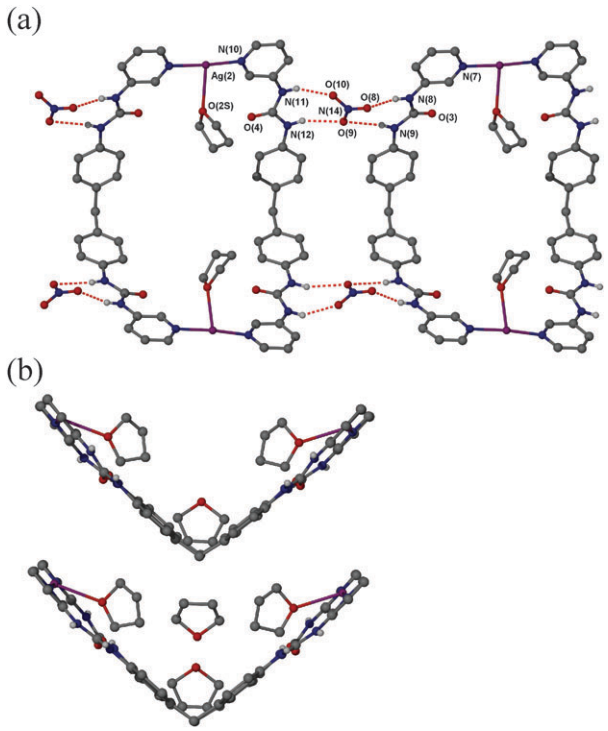

Fig. 20 X-Ray crystal structure of $[\{Ag(\mathbf{L^{10}})(thf)\}_2](NO_3)_2{\cdot}4thf$ (**7**) (a) showing the hydrogen bonding to NO_3^- anions and (b) solvent inclusion within the polar stacks of macrocycles (one of two independent molecules shown).

(crystallographically there are two independent half macrocycles each situated on a mirror plane). The macrocycles are connected *via* hydrogen bonding of the urea NH groups on the exterior of the macrocycle to nitrate anions in two distinct modes. One chain of macrocycles is held together by single hydrogen-bonds between the nitrate and a urea NH groups, both of $R_2^2(8)$ type as in **2**. The other (crystallographically unique) macrocycle chain is held by similar interactions except that the nitrate anion adopts a twisted geometry that could be regarded as a bifurcated combination of $R_2^2(8)$ and $R_2^1(6)$ hydrogen-bonds, albeit with one rather long bifurcated component. The two chains are connected *via* a hydrogen-bond between the oxygen atom of the singly-bonded urea of the first chain with one of the NH groups taking part in a $R_2^1(6)$ hydrogen-bond to a nitrate anion in the second chain. Throughout the structure, there are channels of lattice thf solvent molecules that lie in the spaces between the chains. As well as being similar to **2**, this structure, obtained directly from the gel, is closely analogous to the mixed $MeCN/CHCl_3$ solvate obtained by crystallisation of $AgNO_3/\mathbf{L^{10}}$ from acetonitrile/chloroform.[11] The fact that two similar solvates of the metallomacrocycle can be isolated supports the PXRD data that suggest a compound similar to **2** is found in the xerogel of $\mathbf{L^1}/AgNO_3$. While there is no direct evidence that the crystal structure obtained is identical to that of the gel fibres, the consistent production of metallomacrocycles suggests that they are a common product in these systems and the high degree of solvation and uncommon polar space group ($Pmc2_1$) indicates some difficulty in the packing. Moreover the hydrogen bonding interactions are highly directional along macrocycle chains perpendicular to the stacking direction, consistent with gelation behaviour. The formation of 1D chains in the crystal structures of good gelators is a common feature,[48,49] however in this case the polar ordering of the chains in the crystal is more unusual.

The $AgNO_3/\mathbf{L^{10}}$ gels were characterised by stress sweep rheometry (see ESI†) which showed that they resemble the gels formed by $\mathbf{L^1}$ and $AgNO_3$. G' values are initially high at *ca.* 17 kPa and about half an order of magnitude greater than G''. The elastic modulus decreases rapidly with strain, however.

Attempts to gel solvents other than thf/water with silver tetrafluoroborate and $\mathbf{L^{10}}$ were generally unsuccessful. In the case of acetonitrile, a gelatinous precipitate was obtained while methanol gave a thick slurry at 1 wt%. Increasing the amount of gelator to 1.5 wt% did give an opaque gel, however. Pure acetone, toluene, chloroform thf and water all gave precipitates. Attempts to form gels from other Ag(I) salts as well as a range of copper(II) complexes resulted in the formation of precipitates and no additional gels were isolated.

The anion responsiveness of a silver tetrafluoroborate/$\mathbf{L^{10}}$ gel in aqueous thf was tested by the addition of $CF_3SO_3^-$ anion (as the tetrabutyl ammonium salt). Even though triflate is a relatively non-coordinating anion and is highly unlikely to compete with the pyridyl ligands for the Ag(I) ions, the gel was completely destroyed to give a solution containing a small amount of white precipitate. Addition of BF_4^- did not reverse the process in contrast to related $Cu(BF_4)_2$ switched systems.[14] We interpret these data in terms of the disruption of the urea tape hydrogen bonding motif (that holds the gel fibres together) by competing interactions to triflate and the increased ionic strength of the medium.

Unlike, $\mathbf{L^{10}}$ the tetraethyl analogue, $\mathbf{L^{11}}$ proved to be an effective gelator of chloroform–methanol (1 : 1 v/v) even in the absence of metal salt. The presence of the ethyl groups renders the compound more soluble in organic solvents where hydrogen bonding is more significant. Frequency sweep rheometry established the solid-like nature of the free ligand gel with G' *ca.* 16 kPa (about one order of magnitude greater than G'') and invariant with frequency. An SEM micrograph of the dried xerogel is shown in Fig. 21a revealing a dense, fibrous network. Reaction of $\mathbf{L^{11}}$ with Ag(I) salts $AgBF_4$ and $AgNO_3$ further enhances gel strength consistent with results on $\mathbf{L^1}$ and $\mathbf{L^{10}}$ and also changes the appearance of the xerogel to give narrower, less bunched fibres, Fig. 21b.

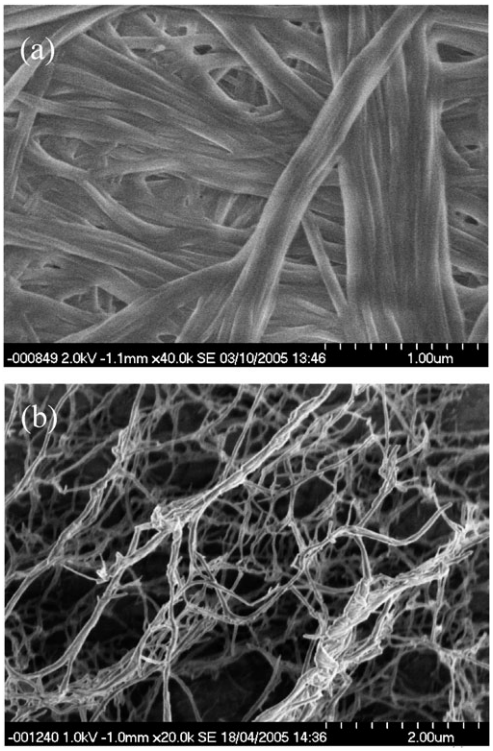

Fig. 21 SEM images of (a) the xerogel of $\mathbf{L^{11}}$ obtained from methanol–chloroform (1 : 1) and (b) xerogel of $\mathbf{L^{11}}/AgBF_4$ (1 : 1) from the same solvent.

Fig. 22 SEM micrograph of a xerogel of $\mathbf{L^{12}}$ and silver(I) tetrafluoroborate (1 : 1) from water/thf (3 : 2).

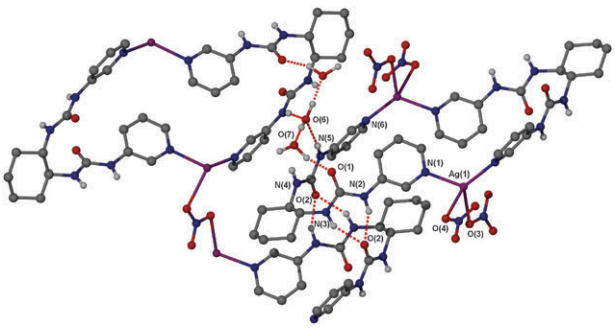

Fig. 23 X-Ray crystal structure of $[\{Ag(\mathbf{L^{12}})\}_2](NO_3)_2{\cdot}3H_2O$ (**8**) showing the water trimer bridging two independent metallomacrocycles, and the urea–urea interaction and nitrate bridging to a further molecule.

Metallogels from $\mathbf{L^{12}}$–$\mathbf{L^{13}}$

Ligand $\mathbf{L^{12}}$ was synthesised from a racemic mixture of *trans*-1,2-diaminocyclohexane. A gel was obtained from a water and thf mixture (3 : 2) of $\mathbf{L^{12}}$ in the presence of one equivalent of silver(I) tetrafluoroborate upon slow evaporation over a few days. SEM was performed on the dried xerogel, and a typical micrograph is shown in Fig. 22. The fibres are over 500 nm long and approximately 50 nm wide. When the metal salt was replaced with silver(I) nitrate in a 1 : 1 mixture of thf and water, the solution initially gelled but upon standing transformed into crystals that were structurally characterised by X-ray crystallography and shown to be another 1 : 1 metallomacrocycle, formula $[\{Ag(\mathbf{L^{12}})\}_2](NO_3)_2{\cdot}3H_2O$ (**8**), Fig. 23. The crystals comprise a racemic mixture of the *R*,*R* and *S*,*S* ligand enantiomers in space group *C*2/*c*. The asymmetric unit contains one half of a metallomacrocycle. The macrocycles in the crystal are subsequently connected to each other through a bifurcated hydrogen-bonding interaction between opposing faces of the urea groups of both sides as well as nitrate bridging. The coordination geometry of the Ag(I) centres is distorted tetrahedral with the metal ion interacting with two nitrate anions as well as two pyridyl groups from two different $\mathbf{L^{12}}$ ligands. The remaining faces of the ligands are hydrogen-bonded to an ordered, three-membered water cluster that connects adjacent chains of macrocycles. The urea oxygen atom forms a single hydrogen bond to a water molecule which is itself hydrogen-bonded to a central water molecule which is shared between the chains. A single N–H group of the urea groups from both chains hydrogen-bonds to the central water molecule. It is noteworthy that crystals **2**, **7** and **8** are all either obtained from gels or in the case of **2** shown by PXRD to resemble the gel phase closely, and all are based on an anion-linked metallomacrocyclic structure that includes significant amounts of solvent of crystallisation.

Ligand $\mathbf{L^{13}}$, *N*,*N*″-pyridine-2,6-diylbis(*N*′-pyridin-3-ylurea), was tested for gelation ability with across a range of ratios of water and thf. In a water and thf mixture (3 : 2) a gel formed at a concentration of 1% w/v in the presence of one equivalent of silver(I) nitrate (see ESI†, Fig. S4). By IR spectroscopy, the N–H bend (Amide II) and C=O peak which occurs at 1547 and 1698 cm^{-1} in the free ligand are shifted to 1558 and 1613 cm^{-1}, respectively, in the xerogel indicating that the urea groups are hydrogen-bonded. T_{gel} was determined to be *ca.* 60 °C, close to the boiling point of thf, by temperature sweep rheometry and the rheological characteristics of the material resemble the gels obtained in this solvent mixture from Ag(I) salts with $\mathbf{L^1}$ and $\mathbf{L^{10}}$, namely a relatively weak gel with a plateau G' value of 4 kPa, *ca.* one order of magnitude greater than G'' but decreasing rapidly with strain and with a relatively low yield point (ESI†, Fig. S5). Frequency sweep rheometry also suggests that G' and G'' decrease gradually with frequency, rather than remaining constant as they would for a true gel.

Experimental

General

^{1}H and ^{13}C-{^{1}H} NMR spectra were measured with either a Bruker Avance NMR spectrometer operating at a proton frequency of 400 MHz or at 200 MHz with a Varian Mercury instrument. Chemical shifts are reported relative to residual solvent peaks. Mass spectra were obtained with a Thermo LTQ FT spectrometer operating by electrospray positive ionization mode. IR spectra were measured with a Perkin-Elmer 100 FT-IR spectrometer, using an uATR attachment. Elemental analysis for carbon, hydrogen and nitrogen was performed on an Exeter analytical E-400 elemental analyser. SEM of chromium-coated freeze-dried samples of gel was performed using an Hitachi S-5200 ultra-high field emission scanning electron microscope. Crystallographic measurements were carried out either with a Nonius KappaCCD or Bruker SMART 1000 or 6000 diffractometers equipped with graphite monochromated Mo-Kα radiation. Data collection temperature was maintained by using an Oxford Cryosystem low temperature device. Integration was carried out either by the Denzo-SMN package or by the Bruker SAINT Software. Data sets were corrected for Lorentz and polarization effects and for the effects of absorption and crystal decay where appropriate. Structures were solved using the direct methods option of SHELXS-97[50] and developed using conventional alternating cycles of least-squares refinement SHELXL-97[51] and difference Fourier synthesis with the aid of the program X-Seed.[52,53] In all cases non-hydrogen atoms were refined anisotropically except for some disordered, while C–H hydrogen atoms were fixed in idealized positions and allowed to ride on the atom to which they were attached. Hydrogen atom thermal parameters were tied to those of the atom to which they were attached. Where possible, non-C–H hydrogen atoms were located experimentally and their positional and isotropic displacement parameters refined. Otherwise a riding model was adopted.

Ligand syntheses

Nicotinoyl azide and ligands **L$^{1-3}$** were prepared as described previously.[29]

***N,N″*-Pentylene-1,5-diylbis(*N′*-pyridin-3-ylurea), L^{4}.** Nicotinoyl azide (1.00 g, 6.75 mmol) was dissolved in dry toluene (50 mL) and stirred at reflux, and the evolution of nitrogen gas monitored. After 2 h, no more gas was evolved and the solution was cooled to room temperature and 1,2-diaminopentane (0.40 mL, 3.40 mmol) was added, precipitating a colourless solid. The suspension was stirred for 15 min, filtered under suction and washed with acetone (2 × 15 mL) to give the product as a white solid 1,5-diaminopentane. Yield: 0.92 g, 2.69 mmol (46%). Mp: 168–170 °C; ^{1}H NMR (DMSO-d_6, 400 MHz, δ/ppm, J/Hz): 8.60 (2H, s, NH), 8.51 (2H, d, J = 2.7, PyH), 8.08 (2H, dd, J = 1.5, 4.6, PyH), 7.87 (2H, ddd, J = 1.5, 2.7, 8.3, PyH), 7.23 (2H, dd, J = 4.6, 8.3), 6.29 (2H, t, J = 6.5, NH), 3.09 (4H, q, J = 6.5, CH_2), 1.45 (4H, m, J = 7.4, CH_2), 1.31 (2H, m, CH_2); ^{13}C{^{1}H} NMR (DMSO-d_6, 100 MHz, δ/ppm): 155.1 (C), 141.9 (CH), 139.5 (CH), 137.2 (C), 124.3 (CH), 123.4 (CH), 39.1 (CH_2), 29.4 (CH_2), 23.7 (CH_2); EI-MS (m/z): 121 [PyNHCO]$^{+}$, 223 [PyNHCONH(CH$_2$)$_5$NH + 2H]$^{+}$, 343 [M + H]$^{+}$, 365 [M + Na]$^{+}$, 707 [2M + Na]$^{+}$; analysis calc. for $C_{17}H_{22}N_6O_2$: C 59.63, H 6.48, N 24.54%; found: C 59.55, H 6.47, N 24.57%; IR (ν/cm^{-1}): 3332 (m, (N–H)$_{str}$), 1627 (strong, sharp, (C═O)$_{str}$), 1556 (strong, sharp, (N–H)$_{def}$).

***N,N″*-Hexylene-1,6-diylbis(*N′*-pyridin-3-ylurea), L^{5}.** Prepared as *N*,*N″*-ethylene-1,2-diylbis(*N′*-pyridin-3-ylurea), using 1,6-diaminohexane. Yield: 0.84 g, 2.36 mmol (70%). Mp: 186–188 °C; ^{1}H NMR (DMSO-d_6, 400 MHz, δ/ppm, J/Hz): 8.59 (2H, s, NH), 8.51 (2H, s, ArH), 8.09 (2H, d, J = 4.8, ArH), 7.87 (2H, d, J = 7.6, ArH), 7.23 (2H, dd, J = 4.8, 8.3, ArH), 6.28 (2H, t, J = 5.3, NH), 3.08 (4H, q, J = 6.4, 12.6, CH_2), 1.46 (4H, br m, CH_2), 1.31 (4H, br m, CH_2); ^{13}C-{^{1}H} NMR (DMSO-d_6, 100 MHz, δ/ppm): 156.6 (C), 142.5 (CH), 139.8 (CH), 137.5 (C), 125.0 (CH), 124.0 (CH), 39.4 (CH_2), 30.0 (CH_2), 26.5 (CH_2); EI-MS (m/z): 179 [M + 2H]$^{2+}$, 357 [M + H]$^{+}$, 379 [M + Na]$^{+}$, 712 [2M + H]$^{+}$, 735 [2M + Na]$^{+}$; analysis calc. for $C_{18}H_{24}N_6O_2$: C 60.66, H 6.79, N 23.58%; found: C 60.10, H 6.84, N 23.47%; IR (ν/cm^{-1}): 3329 (N–H $_{str}$), 1647 (C═O$_{str}$).

***N,N″*-Heptylene-1,7-diylbis(*N′*-pyridin-3-ylurea), L^{6}.** Prepared as *N*,*N″*-ethylene-1,2-diylbis(*N′*-pyridin-3-ylurea), using 1,7-diaminoheptane. Yield: 0.89 g, 2.41 mmol (71%). Mp: 155–157 °C; ^{1}H NMR (DMSO-d_6, 400 MHz, δ/ppm, J/Hz): 8.58 (2H, s, NH), 8.51 (2H, d, J = 2.6, PyH), 8.09 (2H, dd, J = 1.5, 4.7, PyH), 7.87 (2H, ddd, J = 1.5, 2.6, 8.4, PyH), 7.23 (2H, dd, J = 4.7, 8.4, PyH), 6.27 (2H, t, J = 5.6, NH), 3.08 (4H, q, J = 6.5, CH_2), 1.43 (4H, m, J = 6.5, CH_2), 1.29 (6H, m, CH_2-CH_2-CH_2); ^{13}C-{^{1}H} NMR (DMSO-d_6, 100 MHz, δ/ppm): 155.1 (C), 141.9 (CH), 139.5 (CH), 137.2 (C), 124.3 (CH), 123.5 (CH), 39.6 (CH_2), 30.1 (CH_2), 29.2 (CH2), 26.3 (CH_2); EI-MS (m/z): 121 [PyNHCO]$^{+}$, 131 [NH(CH$_2$)$_7$NH + 2H]$^{2+}$, 251 [PyNHCONH(CH$_2$)$_7$NH + 2H]$^{2+}$, 371 [M + H]$^{+}$, 393 [M + Na]$^{+}$, 741 [2M + H]$^{+}$, 763 [2M + Na]$^{+}$. Analysis calc. for $C_{19}H_{26}N_6O_2$: C 61.60, H 7.07, N 21.69%; found: C 61.05, H 6.98, N 22.18%. IR (ν/cm^{-1}): 3332 (m, (N–H)$_{str}$), 1627 (strong, sharp, (C═O)$_{str}$), 1557 (strong, sharp, (N–H)$_{def}$).

***N,N″*-Octylene-1,8-diylbis(*N′*-pyridin-3-ylurea), L^{7}.** Prepared as *N*,*N″*-ethylene-1,2-diylbis(*N′*-pyridin-3-ylurea), using 1,8-diaminooctane. Yield: 1.04 g, 2.70 mmol (80%). Mp: 180–182 °C; ^{1}H NMR (DMSO-d_6, 400 MHz, δ/ppm, J/Hz): 8.58 (2H, s, NH), 8.51 (2H, d, J = 2.6, PyH), 8.10 (2H, dd, J = 1.4, 4.6, PyH), 7.87 (2H, ddd, J = 1.4, 2.6, 8.4, PyH), 7.24 (2H, dd, J = 4.6, 8.4, PyH), 6.27 (2H, t, J = 5.8), 3.08 (4H, q, J = 6.5, CH_2), 1.43 (4H, m, CH_2), 1.29 (6H, m, CH_2); ^{13}C-{^{1}H} NMR (DMSO-d_6, 100 MHz, δ/ppm): 155.1 (C), 142.0 (CH), 139.5 (CH), 137.2 (C), 124.3 (CH), 123.5 (CH), 39.6 (CH_2), 29.6 (CH_2), 28.6 (CH_2), 26.3 (CH_2); EI-MS (m/z): 145, 265, 385 [M + H]$^{+}$, 407 [M + Na]$^{+}$, 769 [2M + H]$^{+}$, 791 [2M + Na]$^{+}$; analysis calc. for $C_{20}H_{28}N_6O_2$: C 62.48, H 7.34, N 21.86%; found: C 62.12, H 7.28, N 21.36%; IR (ν/cm^{-1}): 3336 (m, (N–H)$_{str}$), 1645 (strong, sharp, (C═O)$_{str}$) 1557 (strong, sharp, (N–H)$_{def}$).

***N,N″*-Nonylene-1,9-diylbis(*N′*-pyridin-3-ylurea), L^{8}.** Prepared as *N*,*N″*-ethylene-1,2-diylbis(*N′*-pyridin-3-ylurea), using 1,9-diaminononane. Yield: 1.15 g, 2.88 mmol (85%). Mp: 164–166 °C; ^{1}H NMR (DMSO-d_6, 400 MHz, δ/ppm, J/Hz): 8.58 (2H, s, NH), 8.51 (2H, d, J = 2.6, PyH), 8.09 (2H, dd,

J = 1.4, 4.7, PyH), 7.87 (2H, ddd, J = 1.4, 2.6, 8.3, PyH), 7.23 (2H, dd, J = 4.7, 8.3, PyH), 6.26 (2H, t, J = 5.5, NH), 3.07 (4H, q, J = 6.2, CH_2), 1.42 (4H, m, J = 6.7, CH_2), 1.28 (10H, s, CH_2). ^{13}C-{^{1}H} NMR (100 MHz, DMSO-d_6, 25 °C): 155.1 (C), 141.9 (CH), 139.5 (CH), 137.2 (C), 124.3 (CH), 123.6 (CH), 39.1 (CH_2), 29.6 (CH_2), 29.0 (CH_2), 28.7 (CH_2), 26.3 (CH_2) ppm; EI-MS (m/z): 399 $[M + H]^+$, 421 $[M + Na]^+$, 797 $[2M + H]^+$, 819 $[2M + Na]^+$; analysis calc. for $C_{21}H_{30}N_6O_2$: C 63.29, H 7.59, N 21.09%, found C 62.73, H 7.50, N 20.68%; IR (ν/cm^{-1}): 3336 (m, $(N–H)_{str}$), 1632 (strong, sharp, $(C=O)_{str}$), 1557 (strong, sharp, $(N–H)_{def}$).

***N*,*N*′′-Decylene-1,10-diylbis(*N*′-pyridin-3-ylurea), L[9].** Prepared as *N*,*N*′′-ethylene-1,2-diylbis(*N*′-pyridin-3-ylurea), using 1,10-diaminodecane. Yield: 1.31 g, 3.18 mmol (95%). Mp: 176–178 °C; ^{1}H NMR (DMSO-d_6, 400 MHz, δ/ppm, J/Hz): 8.57 (2H, s, NH), 8.51 (2H, d, J = 2.6, PyH), 8.09 (2H, dd, J = 1.4, 4.6, PyH), 7.87 (2H, ddd, J = 1.4, 2.6, 8.3, PyH), 7.23 (2H, dd, J = 4.6, 8.3, PyH), 6.26 (2H, t, J = 5.5, NH), 3.06 (4H, q, J = 6.8, CH_2), 1.41 (4H, m, J = 6.1, CH_2), 1.27 (12H, s, CH_2); ^{13}C-{^{1}H} NMR (100 MHz, DMSO-d_6, 25 °C): 155.1 (C), 141.9 (CH), 139.4 (CH), 137.2 (C), 124.3 (CH), 123.4 (CH), 39.1 (CH2), 29.6 (CH_2), 29.0 (CH_2), 28.7 (CH_2), 26.3 (CH_2); EI-MS (m/z): 121 $[PyNHCO]^+$, 173, 293, 413 $[M + H]^+$, 435 $[M + Na]^+$, 847 $[2M + Na]^+$; analysis calc. for $C_{22}H_{32}N_6O_2$: C 64.05, H 7.82, N 20.37%; found: C 63.78, H 7.78, N 19.90%; IR (ν/cm^{-1}): 3338 (m, $(N–H)_{str}$), 1648 (strong, sharp, $(C=O)_{str}$), 1562 (strong, sharp, $(N–H)_{def}$).

***N*,*N*′′-Methylenebisphenyl-4,1-diylbis(*N*′-pyridin-3-ylurea), L[10].** Prepared as *N*,*N*′′-ethylene-1,2-diylbis(*N*′-pyridin-3-ylurea), using 4,4′-methylenebisaniline. Yield: 1.05 g, 3.97 mmol (71%). Mp: decomposes above 250 °C; ^{1}H NMR (DMSO-d_6, 400 MHz, δ/ppm, J/Hz): 8.80 (2H, s, NH), 8.73 (2H, s, NH), 8.58 (2H, d, J = 2.5, PyH), 8.17 (2H, d, J = 4.7, PyH), 7.93 (2H, d, J = 8.5, PyH), 7.36 (4H, d, J = 8.4, ArH), 7.30 (2H, dd, J = 4.7, 8.3, PyH), 7.13 (4H, d, J = 8.4, ArH), 3.82 (2H, s, -CH_2-); ^{13}C-{^{1}H} NMR (DMSO-d_6, 400 MHz, δ/ppm): 153.0 (C), 143.2 (CH), 140.3 (CH), 137.5 (C), 136.8 (C), 136.0 (C), 129.4 (CH), 125.8 (CH), 124.2 (CH), 119.2 (CH), 40.3 (CH_2); EI-MS (m/z): 220 $[M + 2H]^{2+}$, 439 $[M + H]^+$, 877 $[2M + H]^+$; analysis calc. for $C_{25}H_{22}N_6O_2$: C 68.48, H 5.06, N 19.17%; found: C 68.43, H 5.03, N 18.88%; IR (ν/cm^{-1}): 3300 (m, $(N–H)_{str}$), 1649 (strong, sharp, $(C=O)_{str}$), 1598 (strong, sharp, $(N–H)_{def}$).

***N*,*N*′′-Methylenebis(3,5-diethylphenyl-4,1-diyl)bis(*N*′-pyridin-3-ylurea), L[11].** 4,4′-Methylenebis(2,6-diethylphenyl isocyanate) (1.00 g, 2.76 mmol) and 3-aminopyridine (0.52 g, 5.50 mmol) were refluxed for 24 h in dichloromethane (50 mL) under constant agitation. The reaction was allowed to cool. The precipitated product was isolated by filtration under pressure and washed with diethyl ether and water, to produce a powder with a slight pink colouration. Yield: 0.911 g, 1.66 mmol, 60%. ^{1}H NMR (DMSO-d_6, J/Hz, δ/ppm): 1.09 (t, 3H, J = 7.6, CH_3); 2.51 (q, 2H, J = 7.6, CH_2); 3.84 (s, 2H, methylene-CH_2); 7.00 (s, 2H, Ar-H); 7.25 (dd, 1H, J = 4.4, 8.0, Py-H); 7.71 (br s, 1H, NH); 7.90 (ddd, 1H, J = 1.6, 2.4, 8.4, Py-H); 8.12 (dd, 1H, J = 1.2, 4.2, Py-H); 8.56 (d, 1H, J = 2.6, Py-H); 8.96 (br s, 1H, NH). ^{13}C-{^{1}H} NMR (DMSO-d_6, δ/ppm). 154.6 (C=O); 143.0 (Py-C); 142.6 (Py-C); 140.2 (Py-C); 125.2 (Py-C); 124.2 (Py-C); 140.6 (Ar-C); 137.8 (Ar-C); 132.3 (Ar-C); 127.0 (Ar-C); 41.5 (methylene-C); 25.1 (ethyl-C); 15.4 (ethyl-C). IR (ν/cm^{-1}) 3287 (NH); 1639 (C=O, urea). ES+-MS: m/z = 551 $[M + H]^+$. Anal. calc. for $C_{33}H_{38}N_6O_2{\cdot}1.5H_2O$: C, 70.84; H, 6.97; N, 15.03%. Found: C, 70.77; H, 6.87; N, 14.86%.

***N*,*N*′′-Cyclohexylene-1,2-diylbis(*N*′-pyridin-3-ylurea), L[12].** Prepared as *N*,*N*′′-ethylene-1,2-diylbis(*N*′-pyridin-3-ylurea), using (±)-*trans*-1,2-diaminocyclohexane. Yield: 0.79 g, 0.22 mmol (66%). Mp: 246–248 °C; ^{1}H NMR (DMSO-d_6, 400 MHz, δ/ppm, J/Hz): 8.70 (2H, s, NH), 8.53 (2H, d, J = 2.6, PyH), 8.06 (2H, dd, J = 1.5, 4.7, PyH), 7.82 (2H, ddd, J = 1.5, 2.6, 8.3, PyH), 7.20 (2H, dd, J = 4.7, 8.3, PyH), 6.23 (2H, d, J = 7.4, NH), 3.44 (2H, m, CH), 1.95 (2H, d, J = 10.5, CH_2), 1.66 (2H, m, CH_2), 1.26 (4H, m, CH_2); ^{13}C-{^{1}H} NMR (DMSO-d_6, 100 MHz, δ/ppm): 155.0 (C), 142.0 (CH), 139.5 (CH), 137.1 (C), 124.4 (CH), 123.3 (CH), 52.7 (CH), 32.7 (CH_2), 24.3 (CH_2); EI-MS (m/z): 178 $[M + 2H]^{2+}$, 355 $[M + H]^+$; analysis calc. for $C_{18}H_{22}N_6O_2$: C 61.00, H 6.26, N 23.71%; found: C 60.90, H 6.24, N 23.76%; IR (ν/cm^{-1}): 3348 (m, $(N–H)_{str}$), 1648 (strong, sharp, $(C=O)_{str}$), 1546 (strong, sharp, $(N–H)_{def}$).

***N*,*N*′′-Pyridine-2,6-diylbis(*N*′-pyridin-3-ylurea), L[13].** Prepared as *N*,*N*′′-ethylene-1,2-diylbis(*N*′-pyridin-3-ylurea), using 2,6-diaminopyridine. Yield: 0.66. g, 1.88 mmol (56%). Mp: 208–210 °C; ^{1}H NMR (DMSO-d_6, 400 MHz, δ/ppm, J/Hz): 9.34 (2H, d, J = 2.8, NH), 8.63 (2H, t, J = 2.4, PyH), 8.08 (2H, dd, J = 1.5, 4.6, PyH), 7.87 (2H, ddd, J = 1.5, 2.7, 8.3, PyH), 7.23 (2H, dd, J = 4.6, 8.3), 6.29 (2H, t, J = 6.5, NH), 3.09 (4H, q, J = 6.5, CH_2), 1.45 (4H, m, J = 7.4, CH_2), 1.31 (2H, m, CH_2); ^{13}C-{^{1}H} NMR (DMSO-d_6, 100 MHz, δ/ppm): 151.1 (C), 141.9 (CH), 139.5 (CH), 137.2 (C), 124.3 (CH), 123.4 (CH), 39.1 (CH_2), 29.4 (CH_2), 23.7 (CH_2); EI-MS (m/z): 207 $[2M + Na]^+$; analysis calc. for $C_{19}H_{28}N_6O_2$: C 59.63, H 6.48, N 24.54%; found: C 59.55, H 6.47, N 24.57%; IR (ν/cm^{-1}): 3494 (m, $(N–H)_{str}$), 1698 (strong, sharp, $(C=O)_{str}$), 1547 (strong, sharp, $(N–H)_{def}$).

Complex syntheses

$\{[Cu(L^1)](NO_3)_2{\cdot}6H_2O\}_n$ (1). *N*,*N*′′-Ethylene-1,2-diylbis-(*N*′-pyridin-3-ylurea) (30 mg, 0.1 mmol) was dissolved in a mixture of thf and water (2 : 3, 5 mL) and added to copper(II) nitrate (23 mg, 0.1 mmol). Crystals formed upon evaporation of the solvent.

Crystallographic data for $C_{14}H_{28}CuN_8O_{14}$: M = 595.98, blue block, 0.21 × 0.12 × 0.10 mm, triclinic, space group $P\bar{1}$ (No. 2), a = 7.4582(11), b = 9.4917(14), c = 9.6997(14) Å, α = 113.399(4)°, β = 106.638(4)°, γ = 98.603(4)°, V = 576.10(15) Å^3, Z = 1, D_c = 1.718 g cm^{-3}, F_{000} = 309, Smart-6K, MoKα radiation, l = 0.71073 Å, T = 120(2) K, $2\theta_{max}$ = 60.0°, 8766 reflections collected, 3371 unique (R_{int} = 0.0400). Final *GooF* = 1.024, R_1 = 0.0449, wR_2 = 0.1043, R indices based on 2609 reflections with $I > 2\sigma(I)$ (refinement on F^2), 193 parameters, 6 restraints. Lp and absorption corrections applied, μ = 1.036 mm^{-1}.

$[\{Ag(L^1)(MeCN)\}_2](NO_3)_2{\cdot}CHCl_3$ (2). *N*,*N*′′-Ethylene-1,2-diylbis(*N*′-pyridin-3-ylurea) (30 mg, 0.10 mmol) was dissolved in a 1 : 1 mixture of MeCN and $CHCl_3$ (4.5 mL) which was then added to solution of silver(I) nitrate (17.0 mg, 0.10 mmol)

in MeOH (3 mL). Crystals formed upon standing which were analysed using X-ray crystallography. Yield: 30.3 mg, 0.05 mmol (48%). Analysis calc. for $C_{43}H_{62}Ag_2N_{20}O_{18}$: C 32.38, H 3.20, N 17.77%; found: C 32.42, H 3.21, N 18.03%; IR (ν/cm^{-1}): 3311 (w, $(N–H)_{str}$), 1681 (strong, sharp, $(C{=}O)_{str}$), 1547 (strong, sharp, $(N–H)_{def}$).

Crystallographic data for $C_{34}H_{40}Ag_2Cl_6N_{16}O_{10}$: M = 1261.26, colourless flat needles, 0.39 × 0.32 × 0.19 mm, triclinic, space group $P\bar{1}$ (No. 2), a = 5.5449(16), b = 13.819(4), c = 15.927(5) Å, α = 85.794(8)°, β = 84.557(8)°, γ = 87.260(7)°, V = 1210.6(6) Å^3, Z = 1, D_c = 1.730 g cm^{-3}, F_{000} = 632, Smart-6K, MoKα radiation, λ = 0.71073 Å, T = 120(2) K, $2\theta_{max}$ = 65.1°, 21 797 reflections collected, 8123 unique (R_{int} = 0.0410). Final *GooF* = 1.038, R_1 = 0.0515, wR_2 = 0.1132, R indices based on 5974 reflections with $I > 2\sigma(I)$ (refinement on F^2), 308 parameters, 0 restraints. Lp and absorption corrections applied, μ = 1.210 mm^{-1}.

{[Ag(L^1)](OAc)·4H$_2$O}$_n$ (4). *N*,*N*″-Ethylene-1,2-diylbis-(*N*′-pyridin-3-ylurea) (15 mg, 0.05 mmol) was dissolved in a 1 : 1 mixture of EtOH and water (3 mL) which was then added to silver(I) acetate (8.3 mg, 0.05 mmol). Upon slow evaporation of the solvent, crystals formed which were analysed using X-ray crystallography. Yield: 10.4 mg, 0.02 mmol (39%). Analysis calc. for $C_{16}H_{27}AgN_6O_8$: C 35.60, H 5.05, N 15.60%; found: C 35.19, H 4.82, N 13.13%. The low value for the nitrogen figure arises from the difficulty in analysing these solvated and unstable crystals. IR (ν/cm^{-1}): 3328 (m, $(N–H)_{str}$), 1669 (strong, sharp, $(C{=}O)_{str}$), 1549 (strong, sharp, $(N–H)_{def}$).

Crystallographic data for $C_{16}H_{27}AgN_6O_8$: M = 539.31, colourless flat needle, 0.21 × 0.16 × 0.10 mm, triclinic, space group $P\bar{1}$ (No. 2), a = 6.8864(5), b = 12.0430(10), c = 13.2699(10) Å, α = 78.535(3)°, β = 77.905(3)°, γ = 78.335(3)°, V = 1039.71(14) Å^3, Z = 2, D_c = 1.723 g cm^{-3}, F_{000} = 552, Smart-6K, MoKα radiation, λ = 0.71073 Å, T = 120(2) K, $2\theta_{max}$ = 65.0°, 15 692 reflections collected, 7102 unique (R_{int} = 0.0452). Final *GooF* = 0.928, R_1 = 0.0407, wR_2 = 0.0775, R indices based on 5317 reflections with $I > 2\sigma(I)$ (refinement on F^2), 312 parameters, 8 restraints. Lp and absorption corrections applied, μ = 1.027 mm^{-1}.

{[Ag(L^1)](SiF$_6$)$_{0.5}$·dmf}$_n$ (5). *N*,*N*″-Ethylene-1,2-diylbis-(*N*′-pyridin-3-ylurea) (15 mg, 0.05 mmol) was dissolved in a 1 : 1 mixture of MeOH and DMF (3 mL) which was then added to silver(I) tetrafluoroborate (9.7 mg, 0.05 mmol). Upon slow evaporation of the solvent, crystals formed which were analysed using X-ray crystallography and proved to be the hexafluorosilicate salt. The source of the silicon is likely to be the glass vessel by reaction with trace HF.

Crystal data for $C_{17}H_{23}AgF_3N_7O_3Si_{0.5}$, M = 552.34, colourless block, 0.15 × 0.13 × 0.09 mm, monoclinic, space group $P2_1/c$ (No. 14), a = 9.0260(8), b = 16.3903(17), c = 14.0277(14) Å, β = 97.969(3)°, V = 2055.2(3) Å^3, Z = 4, D_c = 1.785 g cm^{-3}, F_{000} = 1116, SMART6000, MoKα radiation, λ = 0.71073 Å, T = 120(2) K, $2\theta_{max}$ = 55.0°, 15 292 reflections collected, 4722 unique (R_{int} = 0.0714). Final *GooF* = 0.833, R_1 = 0.0406, wR_2 = 0.0666, R indices based on 2915 reflections with $I > 2\sigma(I)$ (refinement on F^2), 286 parameters, 0 restraints. Lp and absorption corrections applied, μ = 1.073 mm^{-1}.

{[Ag(L^1)](BF$_4$)·MeOH}$_n$ (6). *N*,*N*″-Ethylene-1,2-diylbis-(*N*′-pyridin-3-ylurea) (15 mg, 0.05 mmol) was dissolved in 1 : 1 mixture of MeOH and water (3 mL) which was then added to silver(I) tetrafluoroborate (9.7 mg, 0.05 mmol). Upon slow evaporation of the solvent, crystals formed which were analysed using X-ray crystallography. Yield: 9.3 mg, 0.02 mmol (35%). IR (ν/cm^{-1}): 3361 (m, $(N–H)_{str}$), 1675 (strong, sharp, $(C{=}O)_{str}$), 1539 (strong, sharp, $(N–H)_{def}$).

Crystallographic data for $C_{15}H_{20}AgBF_4N_6O_3$: M = 527.05, colourless needle, 0.18 × 0.12 × 0.11 mm, triclinic, space group $P\bar{1}$ (No. 2), a = 9.1412(13), b = 9.2472(12), c = 11.3257(15) Å, α = 84.346(4)°, β = 84.501(4)°, γ = 87.385(4)°, V = 947.7(2) Å^3, Z = 2, D_c = 1.847 g cm^{-3}, F_{000} = 528, smart-6K, MoKα radiation, λ = 0.71073 Å, T = 120(2) K, $2\theta_{max}$ = 65.9°, 18 399 reflections collected, 6538 unique (R_{int} = 0.0375). Final *GooF* = 0.916, R_1 = 0.0324, wR_2 = 0.0589, R indices based on 5073 reflections with $I > 2\sigma(I)$ (refinement on F^2), 273 parameters, 0 restraints. Lp and absorption corrections applied, μ = 1.134 mm^{-1}.

[{Ag(L^{10})(thf)}$_2$](NO$_3$)$_2$·4thf (7). *N*,*N*″-Methylenebisphenyl-4,1-diylbis(*N*′-pyridin-3-ylurea) was dissolved in a mixture of thf and water (1 : 1) and added to a solution of silver(I) nitrate in thf and water. Upon standing, the solution turned into a clear gel which crystallised. Over time the crystals lose thf solvent and gain moisture from the air. Analysis calc. for $(C_{25}H_{22}AgN_7O_5)_2(H_2O)_3$: C 47.30, H 3.97, N, 15.40%; found: C 47.41, H 3.96, N 14.40%.

Crystal data for $C_{74}H_{92}Ag_2N_{14}O_{16}$, M = 1649.36, colourless needle, 0.20 × 0.05 × 0.05 mm, orthorhombic, space group $Pmc2_1$ (No. 26), a = 24.723(3), b = 17.1669(19), c = 17.388(2) Å, V = 7379.8(15) Å^3, Z = 4, D_c = 1.485 g cm^{-3}, F_{000} = 3424, SMART1000, MoKα radiation, λ = 0.71073 Å, T = 173(2) K, $2\theta_{max}$ = 50.0°, 40 550 reflections collected, 13 276 unique (R_{int} = 0.0619). Final *GooF* = 0.955, R_1 = 0.0617, wR_2 = 0.1551, R indices based on 9254 reflections with $I > 2\sigma(I)$ (refinement on F^2), 972 parameters, 1 restraint. Lp and absorption corrections applied, μ = 0.608 mm^{-1}. Absolute structure parameter[54] = 0.44(4) racemic twin.

[{Ag(L^{12})}$_2$](NO$_3$)$_2$·3H$_2$O (8). *N*,*N*″-Cyclohexane-1,2-diylbis(*N*′-pyridin-3-ylurea) (30 mg, 0.08 mmol) was dissolved in a 1 : 1 mixture of thf and water (3 mL) which was then added to silver(I) nitrate (16.5 mg, 0.08 mmol). Upon slow evaporation of the solvent, crystals formed which were analysed using X-ray crystallography. Yield: 22.2 mg, 0.02 mmol (46%). Analysis calc. for $C_{18}H_{25}AgN_7O_{6.5}$: C 39.22, H 4.57, N 17.78%; found: C 39.33, H 4.46, N 17.58%; IR (ν/cm^{-1}): 3324 (m, $(N–H)_{str}$), 1667 (strong, sharp, $(C{=}O)_{str}$), 1547 (strong, sharp, $(N–H)_{def}$).

Crystallographic data for $C_{18}H_{25}AgN_7O_{6.50}$, M = 551.32, prism colourless, 0.21 × 0.20 × 0.18 mm, monoclinic, space group $C2/c$ (No. 15), a = 24.965(3), b = 8.6312(9), c = 21.090(3) Å, β = 105.509(3)°, V = 4378.9(8) Å^3, Z = 8, D_c = 1.673 g cm^{-3}, F_{000} = 2248, Smart-6K, MoKα radiation, λ = 0.71073 Å, T = 120(2) K, $2\theta_{max}$ = 56.0°, 16 078 reflections collected, 5275 unique (R_{int} = 0.0492). Final

GooF = 0.945, R_1 = 0.0374, wR_2 = 0.0797, *R* indices based on 3762 reflections with $I > 2\sigma(I)$ (refinement on F^2), 306 parameters, 3 restraints. Lp and absorption corrections applied, μ = 0.974 mm^{-1}.

Representative gel preparations

***N*,*N*′′′-Ethylene-1,2-diylbis(*N*′-pyridin-3-ylurea) (L^1) and copper(II) chloride.** *N*,*N*′′-Ethylene-1,2-diylbis(*N*′-pyridin-3-ylurea) (15 mg, 0.05 mmol) was dissolved in thf and water (1 : 1) (1.5 mL) and added to $CuCl_2{\cdot}2H_2O$ (8.5 mg, 0.05 mmol) to yield a clear blue gel. Samples for IR spectroscopic analysis were dried in air. IR (ν/cm^{-1}): 1616 (medium, sharp, $(C{=}O)_{str}$), 1554 (strong, sharp, $(N{-}H)_{def}$).

***N*,*N*′′-Ethylene-1,2-diylbis(*N*′-pyridin-3-ylurea) (L^1) and copper(II) bromide.** *N*,*N*′′-Ethylene-1,2-diylbis(*N*′-pyridin-3-ylurea) (15 mg, 0.05 mmol) was dissolved in thf and water (1 : 1) (1.5 mL) and added to $CuBr_2$ (11.2 mg, 0.05 mmol) to yield a opaque green viscous liquid. Samples for IR spectroscopic analysis were dried in air. IR (ν/cm^{-1}): 1614 (medium, sharp, $(C{=}O)_{str}$), 1555 (strong, sharp, $(N{-}H)_{def}$).

***N*,*N*′′-Ethylene-1,2-diylbis(*N*′-pyridin-3-ylurea) (L^1) and silver(I) nitrate.** *N*,*N*′′-Ethylene-1,2-diylbis(*N*′-pyridin-3-ylurea (15 mg, 0.05 mmol) was dissolved in thf and water (1 : 1) (1.5 mL) and added to solid $AgNO_3$. Upon sonication, the silver nitrate dissolved, and further sonication led to the formation of a clear colourless gel. Samples for IR spectroscopic analysis were dried in air. IR (ν/cm^{-1}): 1614 (medium, sharp, $(C{=}O)_{str}$), 1557 (strong, sharp, $(N{-}H)_{def}$).

***N*,*N*′′-Pyridine-2,6-diylbis(*N*′-pyridin-3-ylurea) (L^{13}) and silver(I) nitrate.** *N*,*N*′′-Pyridine-2,6-diylbis(*N*′-pyridin-3-ylurea) (30 mg, 0.09 mmol) was dissolved in thf and water (3 : 2) (1.5 mL) and added to solid $AgNO_3$ (14. 6 mg, 0.09 mmol). Upon standing after the silver nitrate dissolved, an opaque colourless gel formed. Samples for IR spectroscopic analysis were dried in air. IR (ν/cm^{-1}): 1616 (v. weak, $(C{=}O)_{str}$), 1559 (strong, sharp, $(N{-}H)_{def}$).

***N*,*N*′′-Cyclohexylene-1,2-diylbis(*N*′-pyridin-3-ylurea) (L^{12}) and silver(I) tetrafluoroborate.** *N*,*N*′′-Cyclohexylene-1,2-diylbis(*N*-pyridin-3-ylurea) (30 mg, 0.08 mmol) was dissolved in thf and water (3 : 2) (1.5 mL) and added to solid $AgBF_4$ (16. 5 mg, 0.08 mmol). Upon standing after the silver tetrafluoroborate dissolved, an opaque colourless gel formed. Samples for IR spectroscopic analysis were dried in air. IR (ν/cm^{-1}): 1637 (medium, sharp, $(C{=}O)_{str}$), 1577 (strong, sharp, $(N{-}H)_{def}$).

***N*,*N*′′-Methylenebisphenyl-4,1-diylbis(*N*′-pyridin-3-ylurea) (L^{10}) and silver(I) nitrate.** *N*,*N*′′-Methylenebisphenyl-4,1-diylbis(*N*′-pyridin-3-ylurea) (30 mg, 0.09 mmol) was dissolved in thf and water (3 : 2) (1.5 mL) and added to solid $AgBF_4$ (14.6 mg, 0.09 mmol). Upon standing, the opaque solution transforms into a clear, colourless gel, and after twenty-four hours, the gel decomposes into crystals. Samples of gel for IR spectroscopic analysis were dried in air. IR (ν/cm^{-1}): 1603 (medium, sharp, $(C{=}O)_{str}$), 1543 (strong, sharp, $(N{-}H)_{def}$).

Conclusions

While it is difficult to isolate systematic trends from the data presented, it is clear that addition of metals such as Cu(II) and Ag(I) significantly enhance the gelation ability of pyridyl ureas. This enhancement is thought to be due to a change from urea···pyridyl hydrogen bonding in the free ligands (Fig. 1b) to a metal cross-linked urea tape motif (Fig. 1a), or a metal cross-linked combination of urea tape and urea anion/urea solvent interactions, all of which are featured in the X-ray crystal structures of samples isolated from these gels upon standing or in related mixtures. A particularly common motif is that of an anion-bridged metallomacrocycle and in at least one case PXRD data suggest that a dried xerogel has a similar structure as a fully characterised metallomacrocycle. The metal binding data reported herein show that metal ions can be used to *strengthen* these kinds of supramolecular gels. In combination with earlier work showing that anion binding by urea gelators can *weaken* gelation,[7,8,10,14,15] these phenomena together represent a step along the way to gels with fully chemically tunable rheology.

Acknowledgements

We thank Mrs A. Christine Richardson for SEM support, and the Commonwealth Scholarships Commission and the Engineering and Physical Sciences Research Council for funding.

References

1 L. A. Estroff and A. D. Hamilton, *Chem. Rev.*, 2004, **104**, 1201–1217.
2 D. J. Abdallah and R. G. Weiss, *Adv. Mater.*, 2000, **12**, 1237–1247.
3 M. George and R. G. Weiss, *Acc. Chem. Res.*, 2006, **39**, 489–497.
4 D. K. Smith, in *Organic Nanostructures*, ed. J. L. Atwood and J. W. Steed, Wiley-VCH, Weinheim, 2008, pp. 111–154.
5 P. Dastidar, *Chem. Soc. Rev.*, 2008, **37**, 2699–2715.
6 A. R. Hirst, B. Escuder, J. F. Miravet and D. K. Smith, *Angew. Chem., Int. Ed.*, 2008, **47**, 8002–8018.
7 M.-O. M. Piepenbrock, G. O. Lloyd, N. Clarke and J. W. Steed, *Chem. Rev.*, 2010, **110**, 1960–2004.
8 G. O. Lloyd and J. W. Steed, *Nat. Chem.*, 2009, **1**, 437–442.
9 F. Fages, *Angew. Chem., Int. Ed.*, 2006, **45**, 1680–1682.
10 H. Maeda, *Chem.–Eur. J.*, 2008, **14**, 11274–11282.
11 L. Applegarth, N. Clark, A. C. Richardson, A. D. M. Parker, I. Radosavljevic-Evans, A. E. Goeta, J. A. K. Howard and J. W. Steed, *Chem. Commun.*, 2005, 5423–5425.
12 M.-O. M. Piepenbrock, N. Clarke and J. W. Steed, *Chem. Sci.*, 2010, submitted.
13 M.-O. M. Piepenbrock, N. Clarke and J. W. Steed, *Soft Matter*, 2010, DOI: 10.1039/c0sm00313a.
14 M.-O. M. Piepenbrock, N. Clarke and J. W. Steed, *Langmuir*, 2009, **25**, 8451–8456.
15 M.-O. M. Piepenbrock, G. O. Lloyd, N. Clarke and J. W. Steed, *Chem. Commun.*, 2008, 2644–2646.
16 K. M. Anderson, G. M. Day, M. J. Paterson, P. Byrne, N. Clarke and J. W. Steed, *Angew. Chem., Int. Ed.*, 2008, **47**, 1058–1062.
17 C. E. Stanley, N. Clarke, K. M. Anderson, J. P. Lenthall and J. W. Steed, *Chem. Commun.*, 2006, 3199–3201.
18 M. Yamanaka, T. Nakagawa, R. Aoyama and T. Nakamura, *Tetrahedron*, 2008, **64**, 11558–11567.
19 C. Wang, D. Q. Zhang and D. B. Zhu, *Langmuir*, 2007, **23**, 1478–1482.
20 N. N. Adarsh, D. K. Kumar and P. Dastidar, *Tetrahedron*, 2007, **63**, 7386–7396.

21 S. Arai, K. Imazu, S. Kusuda, I. Yoshihama, M. Tonegawa, Y. Nishimura, K. Kitahara, S. Oishi and T. Takemura, *Chem. Lett*., 2006, **35**, 634–635.
22 Y. Jeong, K. Hanabusa, H. Masunaga, I. Akiba, K. Miyoshi, S. Sakurai and K. Sakurai, *Langmuir*, 2005, **21**, 586–594.
23 F. Fages, F. Vögtle and M. Žinic, *Top. Curr. Chem*., 2005, **256**, 77–131.
24 F. S. Schoonbeek, J. H. van Esch, R. Hulst, R. M. Kellogg and B. L. Feringa, *Chem.–Eur. J*., 2000, **6**, 2633–2643.
25 M. de Loos, A. G. J. Ligtenbarg, J. van Esch, H. Kooijman, A. L. Spek, R. Hage, R. M. Kellogg and B. L. Feringa, *Eur. J. Org. Chem*., 2000, 3675–3678.
26 J. Brinksma, B. L. Feringa, R. M. Kellogg, R. Vreeker and J. van Esch, *Langmuir*, 2000, **16**, 9249–9255.
27 J. van Esch, F. Schoonbeek, M. de Loos, H. Kooijman, A. L. Spek, R. M. Kellogg and B. L. Feringa, *Chem.–Eur. J*., 1999, **5**, 937–950.
28 J. van Esch, R. M. Kellogg and B. L. Feringa, *Tetrahedron Lett*., 1997, **38**, 281–284.
29 P. Byrne, D. R. Turner, G. O. Lloyd, N. Clarke and J. W. Steed, *Cryst. Growth Des*., 2008, **8**, 3335–3344.
30 R. Custelcean, V. Sellin and B. A. Moyer, *Chem. Commun*., 2007, 1541–1543.
31 M. M. Coleman, K. H. Lee, D. J. Skrovanek and P. C. Painter, *Macromolecules*, 1986, **19**, 2149–2157.
32 M. M. Coleman, M. Sobkowiak, G. J. Pehlert, P. C. Painter and T. Iqbal, *Macromol. Chem. Phys*., 1997, **198**, 117–136.
33 P. Terech and R. G. Weiss, *Chem. Rev*., 1997, **97**, 3133–3160.
34 G. A. Buxton and N. Clarke, *Phys. Rev. Lett*., 2007, **98**, 238103.
35 D. R. Turner, B. Smith, A. E. Goeta, I. R. Evans, D. A. Tocher, J. A. K. Howard and J. W. Steed, *CrystEngComm*, 2004, **6**, 633–641.
36 Y. Li, T. Wang and M. Liu, *Tetrahedron*, 2007, **63**, 7468–7473.
37 D. R. Trivedi and P. Dastidar, *Chem. Mater*., 2006, **18**, 1470–1478.
38 G. Cravotto and P. Cintas, *Chem. Soc. Rev*., 2009, **38**, 2684–2697.
39 D. R. Turner, B. Smith, E. C. Spencer, A. E. Goeta, I. R. Evans, D. A. Tocher, J. A. K. Howard and J. W. Steed, *New J. Chem*., 2005, **29**, 90–98.
40 N. Qureshi, D. S. Yufit, J. A. K. Howard and J. W. Steed, *Dalton Trans*., 2009, 5708–5714.
41 R. Custelcean, *Chem. Commun*., 2008, 295–307.
42 S. K. Chandran, R. Thakuria and A. Nangia, *CrystEngComm*, 2008, **10**, 1891–1898.
43 J. M. Russell, A. D. M. Parker, I. Radosavljevic-Evans, J. A. K. Howard and J. W. Steed, *CrystEngComm*, 2006, **8**, 119–122.
44 J. M. Russell, A. D. M. Parker, I. Radosavljevic-Evans, J. A. K. Howard and J. W. Steed, *Chem. Commun*., 2006, 269–271.
45 J. Bernstein, R. E. Davis, L. Shimoni and N.-L. Chang, *Angew. Chem., Int. Ed. Engl*., 1995, **34**, 1555–1573.
46 P. Byrne, G. O. Lloyd, N. Clarke and J. W. Steed, *Angew. Chem., Int. Ed*., 2008, **47**, 5761–5764.
47 P. Byrne, G. O. Lloyd, K. M. Anderson, N. Clarke and J. W. Steed, *Chem. Commun*., 2008, 3720–3722.
48 A. Ballabh, T. K. Adalder and P. Dastidar, *Cryst. Growth Des*., 2008, **8**, 4144–4149.
49 D. Bardelang, F. Camerel, R. Ziessel, M. Schmutz and M. J. Hannon, *J. Mater. Chem*., 2008, **18**, 489–494.
50 G. M. Sheldrick, University of Göttingen, 1997.
51 G. M. Sheldrick, University of Göttingen, 1997.
52 J. L. Atwood and L. J. Barbour, *Cryst. Growth Des*., 2003, **3**, 3–8.
53 L. J. Barbour, *J. Supramol. Chem*., 2001, **1**, 189–191.
54 H. D. Flack, *Acta Crystallogr., Sect. A: Fundam. Crystallogr*., 1983, **39**, 876–881.

